

## Separable Windowed Discrete Time-Frequency Signal Analysis and Processing Techniques for ECG Arrhythmia Signals

S.Sivakumar\*, D.Nedumaran\*\*

\**(P.G. and Research Department of Electronics, Government Arts College, Paramakudi, Tamilnadu, India*

\*\* *(Central Instrumentation and Service Laboratory, University of Madras, Guindy Campus, Chennai, Tamilnadu, India*

### ABSTRACT

A non-stationary ECG signal was analyzed using time-frequency distributions to enhance diagnostic efficiency. The time-frequency distributions were formulated using discrete Wigner-Ville distribution with various windowing techniques. Various time-frequency distributions techniques such as discrete pseudo-Wigner-Ville distribution, separable discrete Lag-Independent smoothed Wigner-Ville distribution, separable discrete Doppler-Independent smoothed Wigner-Ville distribution and separable discrete smoothed pseudo-Wigner-Ville distribution were developed to analyze supra-ventricular and malignant ventricular ECG arrhythmia signals. The performance of the time-frequency distributions was evaluated through energy distribution and time-frequency resolution. The discrete pseudo-Wigner-Ville distribution was computed in the time-lag domain, which gave low resolution in the time-frequency domain. Whereas the Lag-Independent and Doppler independent discrete smoothed Wigner-Ville distributions were computed in the time lag and Doppler-lag domain had resulted in cross-terms problems. But, the discrete smoothed pseudo-Wigner-Ville distribution kernels were served as low-pass filters and could be estimated in the Doppler-lag as well as time-lag domains. The results obtained from this study revealed that the separable discrete smoothed pseudo-Wigner-Ville distribution provided a better resolution in the time-frequency domain and in turn exhibited the shape of the waveform clearly than the other time-frequency distributions. Consequently, the separable kernel time-frequency distributions may be treated as a suitable time-frequency WVD for the detection of the heart rate variability and QRS peak.

**Keywords** - Time-Frequency Distribution, Discrete Wigner-Ville Distribution, Discrete Pseudo Wigner-Ville Distribution, Discrete Smoothed Wigner-Ville Distribution, ECG arrhythmia

Date of Submission: 11-04-2020

Date of Acceptance: 27-04-2020

### I. INTRODUCTION

Most of the real-life signals are non-stationary and multicomponent signals [1]. The electrical activity of the heart generates a pattern of ECG signal during atrial depolarization, ventricular depolarization, and ventricular repolarization and is represented as P-QRS-T complex waves, respectively. The shape, relative position, duration, and amplitude of these waves are considered an important diagnostic tool to a cardiologist in the diagnostic process [2]. Biomedical signals including the ECG signal are characterized as time-varying signal properties, called non-stationary signal in which the components of the signal has time-varying properties occur at different frequencies. Hence, stationary methods are not suitable to analyze time varying characteristic signal. Therefore, the time-variant frequency-selective approach is required for the "time-frequency" analysis of non-stationary signals [3]. Time-frequency techniques are found more suitable, which maps the one-dimensional time-domain signal into two-dimensional time-

frequency representation [4]. They describe signal energy around the instantaneous frequency both on time and frequency spaces [5]. The Wigner-Ville distribution is an important algorithm of time-frequency analysis in biomedical signal processing [6-7]. It has the best time-frequency resolution properties [8-11] and the bilinear nature of Wigner-Ville distribution introduced a cross-term for a multicomponent, non-stationary signal, while preserving most of the signal properties. As a result, many researchers have been experimented the time-frequency distributions to resolve critical technical issues in many areas of science, engineering and technology [12-14].

Wigner-Ville distribution is a primary distribution to form so many classes of bilinear distribution in which windowed Wigner-Ville distribution is one of the recent development in time-frequency distribution [15]. Consequently, this research work concentrated on the analysis of the ECG signal based on windowed Wigner-Ville distribution. Some of the windowing techniques proposed to formulate time-frequency representation

are discrete pseudo-Wigner-Ville distribution (DPWVD), Lag-Independent, Doppler-Independent discrete smoothed Wigner-Ville distributions and separable discrete smoothed pseudo-Wigner-Ville distribution (DSPWVD). To understand the potentially of the proposed methods, the discrete form of time-frequency distributions was computed and compared with Hanning, Hamming, Kaiser and Gaussian windows in time-lag domain and Doppler-lag domain by analyzing the ECG signal for the cardiovascular diseases like supraventricular and malignant ventricular arrhythmia.

This paper is organized as follows: Section 2 presents the analytical signal and signal model of the ECG signal. In Section 3, window characteristics are presented. The methodology to form time-frequency distribution is discussed in Section 4. Simulation results and discussion are presented in Section 5.

## II. ECG ARRHYTHMIA SIGNALS

The abnormal electrical activity of the heart causes an arrhythmia. It is a defect in the conduction of the electrical impulses from the right atria to AV node and AV node to right ventricle at that time the heartbeat may be too fast, too slow or maybe regular or irregular. The abnormal electrical activity of the heart broadly classified as supraventricular arrhythmia and malignant ventricular arrhythmia [16]. In this work, supra-ventricular arrhythmia and malignant ventricular arrhythmia ECG signals were studied. A supraventricular arrhythmia occurs in the right atria due to abnormal impulses arising from the atria. It has irregular shapes of QRS complexes [17]. The malignant ventricular arrhythmia originates from the AV node or ventricle. In this, the QRS complexes are wide and the T wave disappears [18]. The QRS complexes of the abnormal have irregular shapes and changes over time.

The ECG arrhythmia signals are obtained from the MIT BIH arrhythmia database [19]. The signals were sampled at 360Hz. This time-domain signal is represented by  $x[n]$  is a real, causal and band-limited signal. It has both positive and negative frequency components introducing aliasing. The aliasing can be avoided by a technique called analytical signal representation.

### 2.1 Analytical Signal and Hilbert Transformation

In order to get alias-free signal, the real-valued signal  $x[n]$  is converted into an analytical complex-valued signal using Hilbert transform defined in Eq. : (1).

$$z[n] = x[n] + jH(x[n]) \quad (1)$$

where  $H(x[n])$  is a Hilbert transform of the real-valued signal  $x[n]$  and  $z[n]$  is an analytical signal of

the analytical associate  $x[n]$ . It is also calculated in frequency domain using Fourier transform [20-21].

### 2.2. Signal Modeling

Before analyzing any signal using time-frequency distribution, the signal must be checked for mono-component or multi-component signal in order to create a model of the signal for analysis. After computing the analytical signal, the signal model is derived by extracting instantaneous amplitude (IA), instantaneous phase (IP), instantaneous frequency (IF) and group delay (ID). In the case of ECG arrhythmia signal, the bandwidth and time spread of the ECG arrhythmia signal are calculated and determined as a multicomponent signal and then modeled as AM-FM signal model described in [22]. It is represented by Eq. : (2)

$$z(n) = \sum_{k=1}^{N_c} z_k = \sum_{k=1}^{N_c} m_k(n) a_k(n) \cos(\phi_k(n)) w(n) \quad (2)$$

## III. AN ANALYSIS OF WINDOW FUNCTION

The process of multiplying the measured signal with a smoothly ending function is called window function. The window function is used to reduce the spectral leakage [23], detect the desired signal and get high resolution by smoothing the time and frequency components. The DPWVD and DSPWVD have employed several window functions to increase or optimize the time and frequency resolutions for a particular application. In this work, the DPWVD and DSPWVD are used and their characteristics are studied using the following window functions.

The rectangular window sequence is represented in Eq. : (3)

$$W_R(n) = \begin{cases} 1 & \text{for } -\frac{N}{2} \leq n \leq \frac{N}{2} \\ 0 & \text{otherwise} \end{cases} \quad (3)$$

The Hanning window sequence is given by the Eq. :(4)

$$W_{Hn}(n) = \begin{cases} 0.5 + 0.5 \cos \left[ \frac{2\pi n}{N} \right] & \text{for } -\frac{N}{2} \leq n \leq \frac{N}{2} \\ 0 & \text{otherwise} \end{cases} \quad (4)$$

The Hamming window sequence is given by the Eq. : (5)

$$W_{Hm}(n) = \begin{cases} 0.54 + 0.46 \cos \left[ \frac{2\pi n}{N} \right] & \text{for } -\frac{N}{2} \leq n \leq \frac{N}{2} \\ 0 & \text{otherwise} \end{cases} \quad (5)$$

The Kaiser Window sequence is defined in Eq. :(6)

$$W_K(n) = \frac{I_0 \left\{ \pi \alpha \sqrt{1 - \left[ \frac{2n}{N-1} - 1 \right]^2} \right\}}{I_0(\pi \alpha)}, \text{ for } -N \leq n \leq N \quad (6)$$

The Gaussian window sequence is expressed in Eq. :(7)

$$W_G(n) = \exp \left[ -\frac{1}{2} \left( \frac{n - (N-1)/2}{\sigma(N-1)/2} \right)^2 \right] \quad (7)$$

### 3.1. Window Selection

Window selection is determined by three parameters viz., main lobe width, side lobe level, and Equivalent Noise Band Width (ENBW). The desirable characteristics of a window are mainly depends on the width of the main lobe, i.e., the frequency resolution mainly depends on the main lobe width[24], for example, if the main lobe width is narrow it gives high-frequency resolution and contain most of the energy. The main lobe width is the measure of the main lobe width at -3db below the main lobe peak. Side lobe occurs at either side of the main lobe. It is measured in dB relative to the peak of the main lobe. When the side lobe level decreases it increases the detection ability. ENBW is calculated as a ratio of inherent power gain over coherent power gain as given in Eq. :(8), (9) and (10).

$$\text{Inherent Power Gain} = \frac{1}{N} \sum_{i=1}^N w(i)^2 \quad (8)$$

$$\text{Coherent Power Gain} = \left[ \frac{1}{N} \sum_{i=1}^N w(i) \right]^2 \quad (9)$$

$$\text{ENBW} = \frac{\text{Inherent Power Gain}}{\text{Coherent Power Gain}} \quad (10)$$

The shape and size of these windows are shown in the Fig.1. The frequency response of the window length is 64 as shown in the Fig. 2. The equivalent noise band width (ENBW) value of each window is calculated and given in the Table 1.

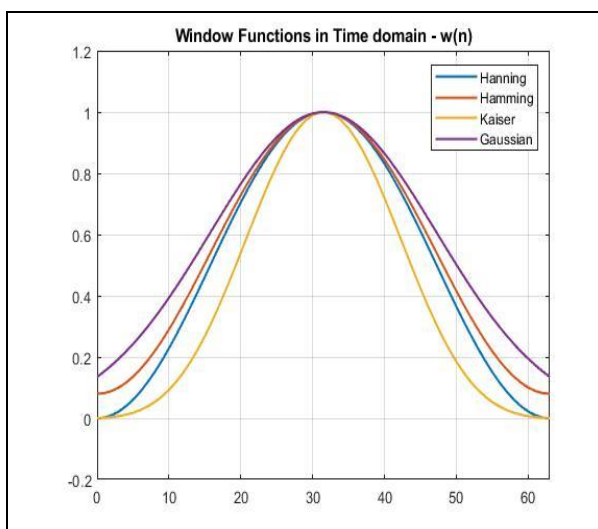


Fig. 1 Window function shape in Time Domain

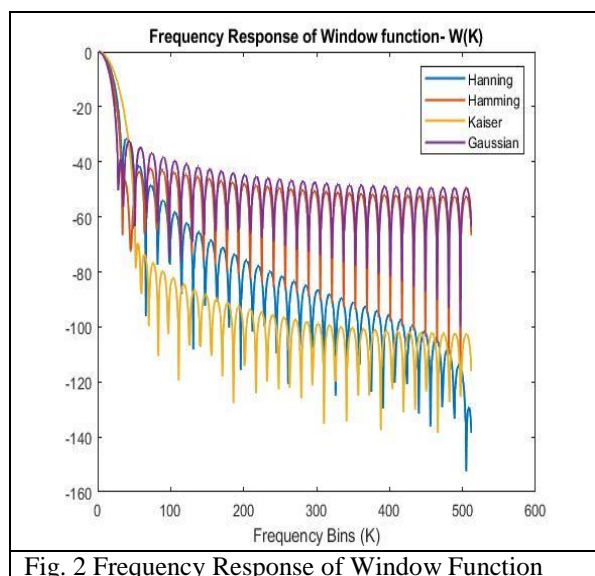


Fig. 2 Frequency Response of Window Function

Table 1: Window selection parameters

S.No.	Window Type	Side lobe Level	3dB bandwidth	ENBW
1	Rectangular	-13.2	0.87	1
2	Hanning	-32	1.47	1.5
3	Hamming	-43.5	1.35	1.36
4	Kaiser	-69.6	1.73	1.82
5	Gaussian	-32.3	1.15	1.23

## IV. FORMULATION OF TIME-FREQUENCY DISTRIBUTIONS

The Wigner-Ville distribution with a smoothing window formulated the time-frequency distribution to realize and implement in the hardware and software environment for a particular application. The discrete version of the equation is formulated as [25]:

$$\rho[n, k] = 2 \text{DFT}_{n \rightarrow k} \left\{ G[n, m]_n^* \left( z[n+m] z^*[n-m] \right) \right\} \quad (11)$$

where  $n$  is the time index,  $m$  is the lag index,  $k$  is the frequency index,  $z[n]$  is an analytical signal of analytical associate  $x[n]$ ,  $G[n, m]$  is the window function in time-lag domain and  $\rho[n, k]$  is the time-frequency distribution in the time-frequency domain.

$$k_z[n, m] = z[n+m] z^*[n-m] \quad (12)$$

where Eq. : (12) is an instantaneous auto-correlation function (IACF) in time-lag domain.

### 4.1 Discrete Wigner-Ville Distribution

To form the discrete Wigner-Ville distribution, the window function in the Eq. (11) is equal to a rectangular window [26-27] and therefore

$$G[n, m] = \delta[n] = 1 \quad (13)$$

Hence, only the instantaneous auto correlation function (IACF) itself formed the Wigner-Ville distribution [28] and is given by Eq. :(14)

$$DWVD[n,k]=2 \sum_{m=-\infty}^{\infty} z[n+m]z^*[n-m]e^{(-j\frac{2\pi}{N}km)} \quad (14)$$

The instantaneous autocorrelation is performed on the analytical signal  $z[n]$  and its conjugate value  $z^*[n]$  in the time-lag domain is called the signal kernel. Here,  $n$  is the discrete-time index  $0 \leq n \leq N$ ,  $m$  is the lag index  $-N \leq m \leq N$  and  $k$  is the frequency index  $0 \leq k \leq N$ . After performing convolution on time-lag domain, the processed value of  $k_z [n, m]$  is transferred from time-lag domain to time-frequency domain by taking Fourier transform to get DWVD in time-frequency domain.

$$DWVD[n,k]=2 DFT \sum_{m=-\infty}^{\infty} k_z[n,m]e^{(-j\frac{2\pi}{N}km)} \quad (15)$$

#### 4.2 Discrete Pseudo-Wigner-Ville Distribution

The Wigner-Ville distribution introduced a cross-term because the Fourier transform on the instantaneous autocorrelation function over the lag make the Wigner-Ville distribution as a non-causal distribution. It is not suitable for real-time signal processing. To minimize the cross term and make suitable for real-time application, applying the Wigner-Ville distribution to a windowed version of the signal [29-30]. Setting the time-lag window  $G(n, m) = \delta(n)h(m)$  [31]. The PWVD of a discrete signal with a finite length lag window is given by,

$$DPWVD[n,k]= \sum_{m=-\frac{N}{2}}^{\frac{N}{2}} h[m]z[n+m]z^*[n-m]e^{-j\frac{2\pi}{N}km} \quad (16)$$

where  $h[m]$  is a real-valued frequency smoothing window with odd length  $2N-1$  [32]. Due to the window function, Fourier transforms consider only the signal components in the instantaneous autocorrelation function. Thus, the Fourier transform over lag will represent only the frequency components and reduces the cross-term. The effect of the windowing is to smear the signal in a frequency direction without affecting the time resolution. Hanning, Hamming, Kaiser, and Gaussian windows are chosen [33-34] to minimize interference and improve the frequency resolution.

#### 4.3 Formation of Separable Time-Frequency Distribution

The kernel is represented in a time-lag domain as  $g[n, m]$  where  $n$  is the time index and  $m$  is the lag index. To reduce the cross term, the kernel in the

time-lag domain is transformed to the Doppler-lag domain by taking DFT of  $n$  and represented as  $g[u, m]$ . Now, the kernel is separated as Doppler function  $G_1[u]$  and lag function as  $g_2[m]$ . Therefore, the separable kernel is equal to the product of Doppler function and lags function in Doppler-lag domain [35-37] and is given by,

$$g[u, m]=G_1[u]g_2[m] \quad (17)$$

The dependence on the type of separable kernel  $G_1[u]$  and  $g_2[m]$  act as either low pass filter or all-pass filter.

The separable kernel can be divided into three types [38]

1. Lag-Independent kernel,  $G_1[u]$  act as a low pass filter and  $g_2[m]$  act as an all-pass filter in which  $g_2[m] = 1$ . The product of  $G_1[u]$  and  $g_2[m]$  forms the Lag-Independent kernel.
2. Doppler-Independent kernel,  $g_2[m]$  act as a low pass filter and  $G_1[u]$  acts as an all-pass filter in which  $G_1[u] = 1$ . The product of  $g_2[m]$  and  $G_1[u]$  forms the Doppler-Independent kernel.
3. To control both on time and frequency domains,  $G_1[u]$  and  $g_2[m]$  are used as a low pass filter. The product of these two low pass filters forms a kernel.

#### 4.3.1 Discrete Lag-Independent Smoothed Wigner-Ville Distribution:

The kernel is used in the Doppler-lag domain is a function of Doppler only [38-39] and it is defined as

$$g[u, m]=G_1[u] \quad (18)$$

Then, the discrete Lag-Independent smoothed Wigner-Ville distribution (DLISWVD) is formed by introducing Doppler window in the Wigner-Ville distribution and is defined as

$$DLISWVD=W_z[n, k] * g_1[n] \quad (19)$$

and it is expanded using the equation (11), we get,

$$DLISWVD(n, k)= \sum_{m=-\frac{N}{2}}^{\frac{N}{2}} g_1[n]z(n+m)z^*(n-m)e^{-j\frac{2\pi}{N}km} \quad (20)$$

where  $g_1[n]=DFT_{n \rightarrow u} G_1[u]$ , several quadratic

time-frequency distributions on Lag-Independent kernels are proposed such as Hanning, Hamming, Kaiser, and Gaussian windows. Expression of these windows in the Doppler-lag domain and its dual in time-frequency domain [38] are given below.

$$W_{Hann}[u]=0.5+0.5 \cos \left[ \frac{2\pi u}{N} \right] \quad (21)$$

$$W_{Hamm}[u]=0.5+0.46 \cos \left[ \frac{2\pi u}{N} \right] \quad (22)$$

$$W_K(u) = \frac{I_0 \left\{ \pi\alpha \sqrt{1 - \left[ \frac{2u}{N-1} - 1 \right]^2} \right\}}{I_0(\pi\alpha)} \quad (23)$$

$$W_G(u) = \exp \left[ -\frac{1}{2} \left( \frac{u - (N-1)/2}{\sigma(N-1)/2} \right)^2 \right] \quad (24)$$

In  $g[n, m]$ , the time  $n$  is transformed to the Doppler domain by taking DFT and it is represented as  $g[u, m]$ . It is separated as a low pass filter  $G_1[u]$  and all-pass filter  $g_2[m]=1$ . Then, perform the instantaneous autocorrelation on the window  $G[u]$  in the ambiguity domain and take IDFT and DFT back to get time-frequency distribution in the time-frequency domain.

The kernel is used in the Doppler-lag domain is a function of the lag only [38] and it is defined as

$$g[u, m] = g_2[m] \quad (25)$$

Then, the discrete Doppler-Independent smoothed Wigner-Ville distribution (DDISWVD) is formed by introducing lag window in the Wigner-Ville distribution and is defined as

$$DDISWVD = W_z[n, k] * G_2[k] \quad (26)$$

and it is expanded using the equation (11), we get,

$$DDISWVD(n, k) = \sum_{m=-\frac{N}{2}}^{\frac{N}{2}} g_2[m] z(n+m) z^*(n-m) e^{-j\frac{2\pi}{N}km} \quad (27)$$

where  $g_2[m] = \underset{m \rightarrow k}{DFT} G_2[k]$ , several quadratic

time-frequency distributions on Doppler-Independent kernels are proposed such as Hanning, Hamming, Kaiser, and Gaussian windows. Expression of these windows in the Doppler-lag domain and its dual in time-frequency domain [38] are given below.

$$W_{Hann}[m] = 0.5 + 0.5 \cos \left[ \frac{2\pi m}{N} \right] \quad \text{for } 0 \leq m \leq \frac{1}{2} \quad (28)$$

$$W_{Hamm}[m] = 0.5 + 0.46 \cos \left[ \frac{2\pi m}{N} \right] \quad \text{for } 0 \leq m \leq \frac{1}{2} \quad (29)$$

$$W_K(m) = \frac{I_0 \left\{ \pi\alpha \sqrt{1 - \left[ \frac{2m}{N-1} - 1 \right]^2} \right\}}{I_0(\pi\alpha)} \quad \text{for } 0 \leq m \leq \frac{1}{2} \quad (30)$$

$$W_G(m) = \exp \left[ -\frac{1}{2} \left( \frac{m - (N-1)/2}{\sigma(N-1)/2} \right)^2 \right] \quad \text{for } 0 \leq m \leq \frac{1}{2} \quad (31)$$

In  $g[n, m]$ , the time  $n$  is transformed to the Doppler domain by taking DFT and it is represented as  $g[u, m]$ . It is separated as a low pass filter  $g_2[m]$  and all-pass filter  $G_1[u]=1$ . Then, perform the instantaneous autocorrelation on the window  $g_2[m]$  in the ambiguity domain and take IDFT and DFT back to get TFD in the time-frequency domain.

### 4.3.3 Discrete Smoothed Pseudo-Wigner-Ville Distributions (DSPWVD)

The Lag-Independent and Doppler-Independent kernels improve the frequency resolution only. To get high resolution on time and frequency domains, smoothing window function is inserted in the SWVD. The SPWVD has a separable kernel given by Eq. (32).

$$g(u, m) = G_1[u] g_2[m] \quad (32)$$

where  $g_2[m] = g_2 \left| \frac{m}{2} \right|^2$ ,  $G_1(u)$  is the smoothing

window with odd length  $2M-1$  and  $g_2(m)$  is the analysis window with odd length  $2N-1$ . These  $G_1[u]$  and  $g_2[m]$  windows are used as low pass filters. The product of these two low pass filters forms a kernel to suppress spurious peaks and to obtain a high time-frequency resolution. The discrete version of the Smoothed Pseudo-Wigner-Ville distribution [40-41] is given by Eq. (33).

$$DSPWVD(n, k) = \sum_{m=-N+1}^{N-1} g_2(m) g_2(-m) \left[ \sum_{u=-M+1}^{M-1} G_1(u) z(n+u+m) z^*(n+u-m) \exp \left( -j\frac{2\pi}{N}km \right) \right] \quad (33)$$

In this, the Gaussian window was used as a smoothing window  $G_1[u]$ , the Hanning, Hamming and Kaiser Windows were used as an analysis window  $g_2[m]$ .

## V. RESULTS AND DISCUSSION

The time-domain ECG supraventricular and malignant ventricular signals are shown in the Figs.3 and 4, respectively. These signals are a real-valued signal and converted into an analytical signal. These signals were analyzed using the proposed time-frequency distributions and are presented as case studies (case 1, case 2, case 3 and case 4).

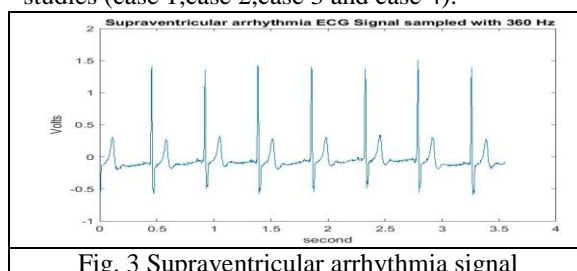


Fig. 3 Supraventricular arrhythmia signal

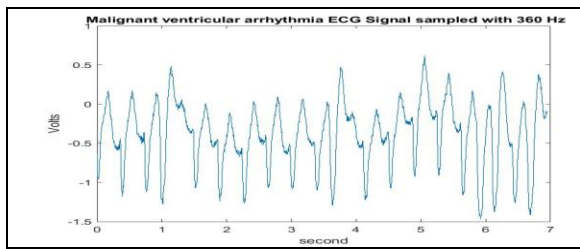


Fig. 4 Malignant ventricular arrhythmia signal  
 Case 1: Analysis of ECG arrhythmia using discrete pseudo-Wigner-Ville distribution

The supraventricular ECG arrhythmia signal was analyzed using discrete pseudo Wigner-Ville distribution by implementing Hanning, Hamming, Kaiser and Gauss windows. These windows smeared the discrete Pseudo -Wigner-Ville distribution in frequency direction in order to improve the frequency resolution without affecting the time resolution. Then, the windows were optimized to get optimum frequency resolution and time resolution and are given in Table 2. The supraventricular arrhythmia was mapped and analyzed by energy distributions of Hanning, Hamming, Kaiser and Gauss windows in the time-frequency domain and are shown in Figs.(5-8), respectively.

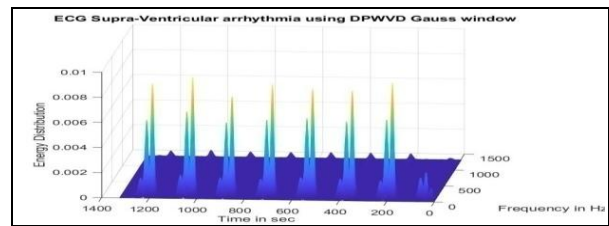


Fig.8 Energy Distribution plot of the Supraventricular Arrhythmia DPWVD signal using Gaussian window function

The performance of these four windows was compared, in which discrete pseudo-Wigner-Ville distribution (DPWVD) with the Gaussian window detected the QRS and T wave multicomponent signal. Further, it exhibited the energy distributed around the instantaneous frequencies with optimum time-frequency resolution.

The malignant ventricular ECG arrhythmia signal was analyzed using discrete pseudo-Wigner-Ville distribution (DPWVD) by implementing Hanning, Hamming, Kaiser and Gauss windows. These windows smeared the discrete pseudo-Wigner-Ville distribution in frequency direction in order to improve the frequency resolution as shown in Figs. (9-12). These windows were optimized to get optimum frequency resolution and time resolution and are given in Table 3.

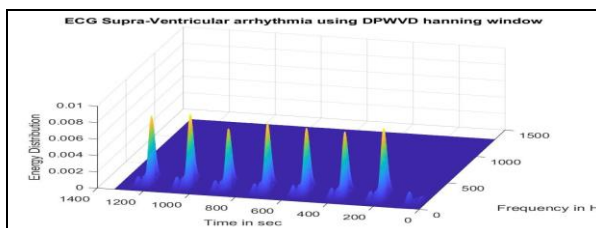


Fig.5 Energy Distribution plot of the Supraventricular Arrhythmia signal using DPWVD Hanning window function

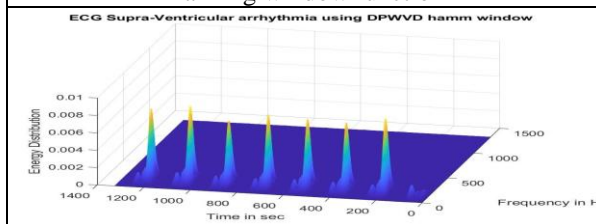


Fig. 6 Energy Distribution plot of the Supraventricular Arrhythmia signal using DPWVD Hamming window function

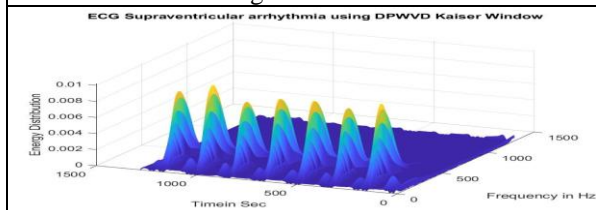


Fig. 7 Energy Distribution plot of the Supraventricular Arrhythmia signal using DPWVD Kaiser window function

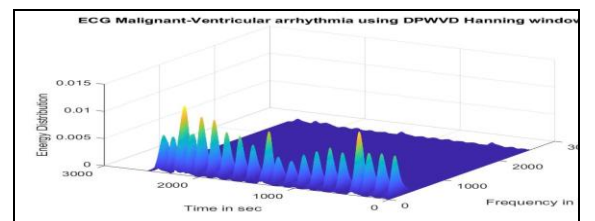


Fig. 9 Energy Distribution plot of the Malignant ventricular arrhythmia signal using DPWVD Hanning window function

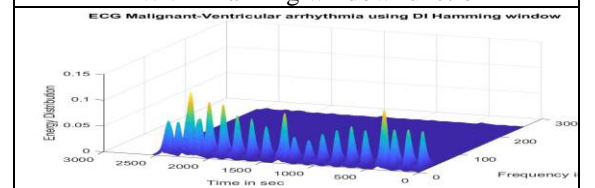


Fig. 10 Energy Distribution plot of the Malignant ventricular arrhythmia signal using DPWVD Hamming window function

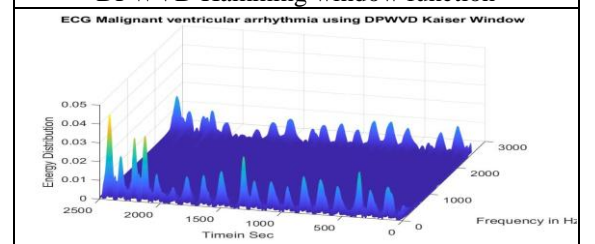
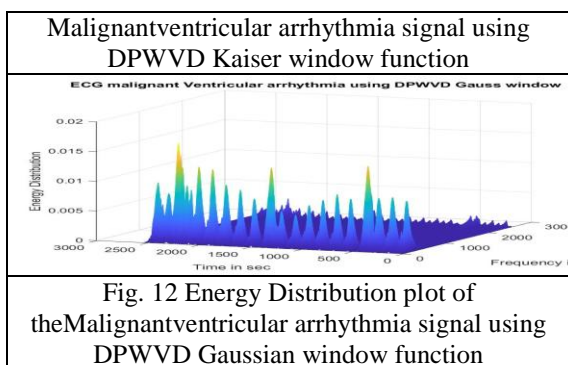


Fig. 11 Energy Distribution plot of the



The analysis results of these four types of windows using DPWVD exhibited that the Gaussian window resolved the multi-components of the QRS and T waves very well than the other windows. Consequently, the energy distributed around the instantaneous frequencies was found to be resolved low in the time-frequency domain.

Case 2: Analysis of ECG arrhythmia signals using Lag-Independent DSWVD

The supra-ventricular ECG arrhythmia signal was analyzed using discrete Lag-Independent smoothed Wigner-Ville distribution (LI-DSWVD) by implementing Hanning, Hamming, Kaiser and Gauss windows and their corresponding energy distribution are shown in the Figs.(13-16), respectively. The windows were optimized to get maximum resolution in frequency and time domain and are summarized in Table 2.

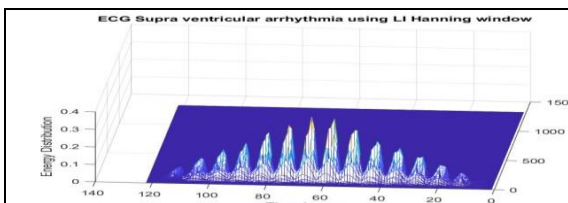


Fig. 13 Energy Distribution plot of the Supraventricular arrhythmia signal using LI-DSWVD Hanning window function

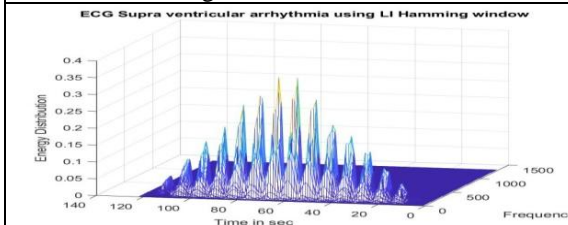


Fig. 14 Energy Distribution plot of the Supraventricular arrhythmia signal using LI-DSWVD Hamming window function

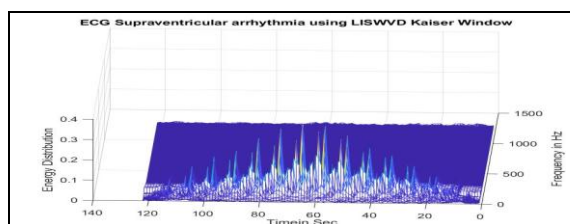


Fig. 15 Energy Distribution plot of the Supraventricular arrhythmia signal using LI-DSWVD Kaiser window function

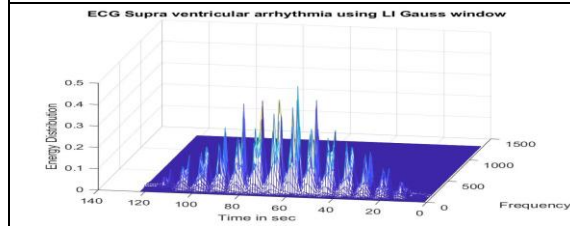


Fig. 16 Energy Distribution plot of the Supraventricular arrhythmia signal using LI-DSWVD Gaussian window function

From the Figs. (13-16), it is clear that the energy distribution of the lag independent window decreases the frequency resolution, due to the presence of the cross-terms in the frequency domain.

Similarly, the malignant ventricular ECG arrhythmia signal was examined in the discrete Lag-Independent smoothed Wigner-Ville distribution for the four window functions such as Hanning, Hamming, Kaiser and Gaussian and their corresponding time-frequency distributions are shown in the Figs. (17-20), respectively, after optimizing the respective window functions and are summarized in Table 3.

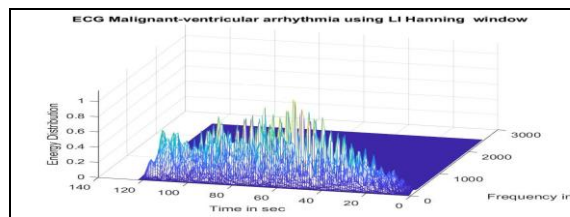


Fig. 17 Energy Distribution plot of the Malignant ventricular arrhythmia signal using LI-DSWVD Hanning window function

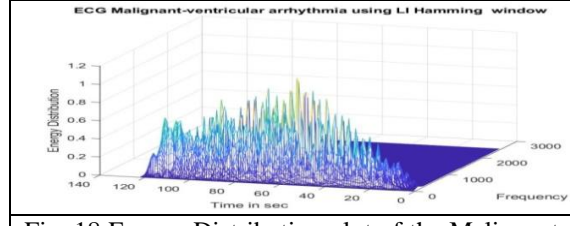


Fig. 18 Energy Distribution plot of the Malignant ventricular arrhythmia signal using LI-DSWVD Hamming window function

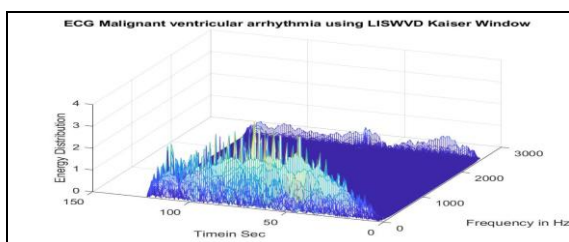


Fig. 19 Energy Distribution plot of the Malignant ventricular arrhythmia signal using LI-DSWVD Kaiser window function

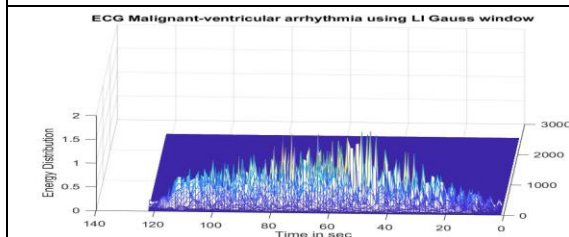


Fig. 20 Energy Distribution plot of the Malignant ventricular arrhythmia signal using LI-DSWVD Gaussian window function

From the energy distribution plots of the malignant ventricular arrhythmia, the time-frequency distribution introduced cross-terms both in the Doppler as well as lag directions. This result shows that the time-frequency distribution had no frequency and time resolution.

Case 3: Analysis of ECG arrhythmia using Doppler-Independent DSVD

The supraventricular ECG arrhythmia signal was tested in the discrete Doppler-Independent smoothed Wigner-Ville distribution for the four window functions viz., Hanning, Hamming, Kaiser and Gaussian and their corresponding energy distribution plots in the time-frequency domains are shown in the Figs. 21-24, respectively. The optimized windows to get better frequency and time resolution are given in Table 2.

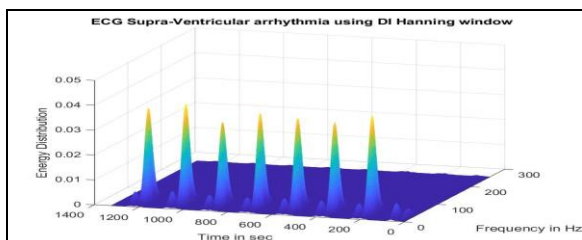


Fig. 21 Energy Distribution plot of the Supraventricular arrhythmia signal using DI-DSWVD Hanning window function

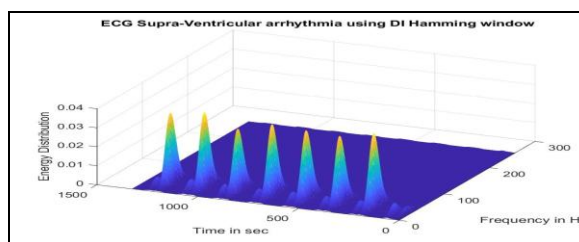


Fig. 22 Energy Distribution plot of the Supraventricular arrhythmia signal using DI-DSWVD Hamming window function

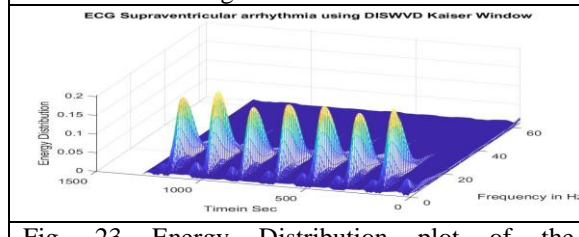


Fig. 23 Energy Distribution plot of the Supraventricular arrhythmia signal using DI-DSWVD Kaiser window function

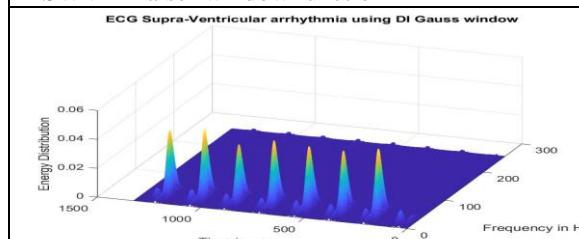


Fig. 24 Energy Distribution plot of the Supraventricular arrhythmia signal using DI-DSWVD Gaussian window function

All the four windows with the DI-DSWVD detected the QRS peaks and their change in shape with high energy distribution and better resolution in the time-frequency domain. Further, the wave was noticed with low energy distribution.

Similarly, the malignant ventricular ECG arrhythmia signal was tested in the DI-DSWVD algorithm using the four window functions viz., Hanning, Hamming, Kaiser and Gaussian and their energy distribution in the time-frequency domain are in the Figs. 25-28, respectively. The results were obtained for the optimized window functions given in Table 3.

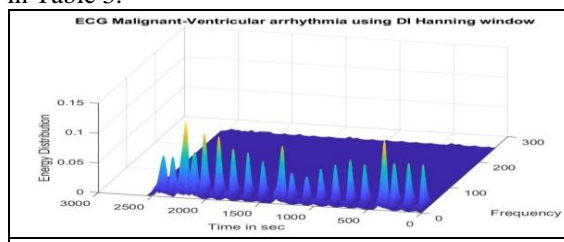


Fig. 25 Energy distribution plot of the Malignant ventricular arrhythmia signal using DI-DSWVD Hanning window function

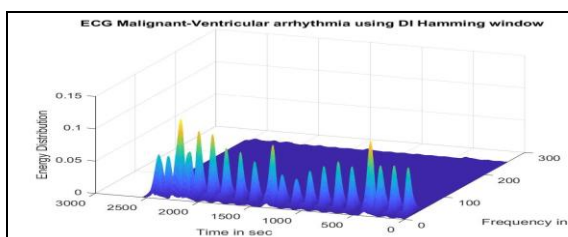


Fig. 26 Energy distribution plot of the Malignant ventricular arrhythmia signal using DI-DSWVD Hamming window function

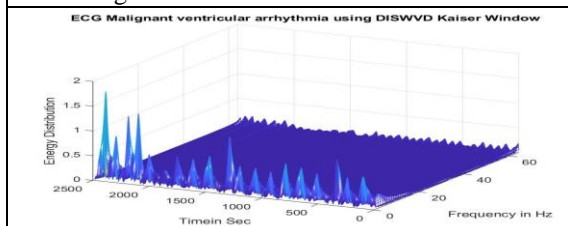


Fig. 27 Energy distribution plot of the Malignant ventricular arrhythmia signal using DI-DSWVD Kaiser window function

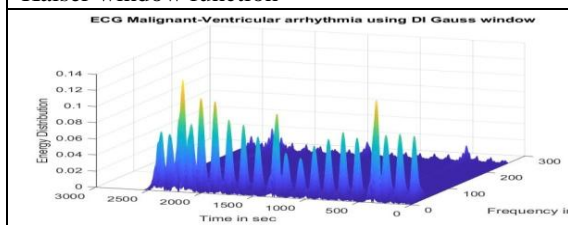


Fig. 28 Energy distribution plot of the Malignantventricular arrhythmia signal using DI-DSWVD Gaussian window function

Even though the Hanning, Hamming and Gauss windows detected the variations in QRS peak with high energy distribution, wave shape and better resolution in time-frequency domain, still the cross-term influence was observed in the energy distribution plots.

#### Case 4: Analysis of ECG arrhythmia signals using DSPWVD

The supraventricular arrhythmia signal was tested in the discrete smoothed pseudo-Wigner-Ville distribution using Hanning, Hamming and Kaiser as analysis window functions and Gauss window as a smoothing window function. The corresponding energy distribution and contour plots are shown in Figs. 29-34. The windows used in this study were optimized for better time-frequency resolution as per the values summarized in Table 2.

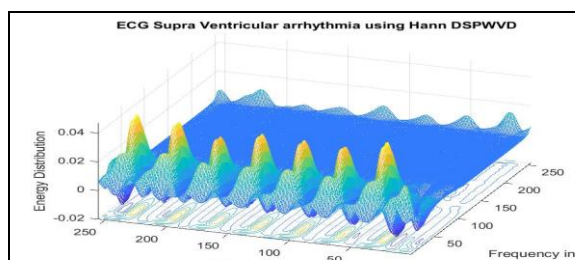


Fig. 29 Energy Distribution Plot of the Supraventricular arrhythmia signal using DSPWVD with Gaussian and Hanning window functions

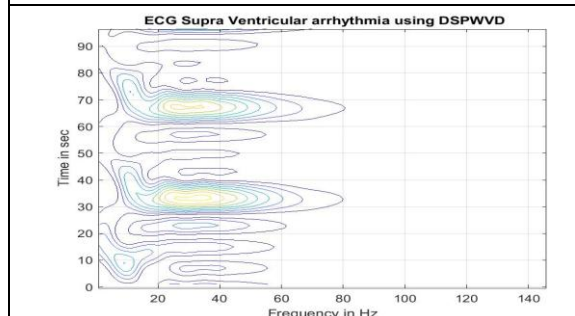


Fig. 30 Contour plot of the Supraventricular arrhythmia signal using DSPWVD with Gaussian and Hanning window functions

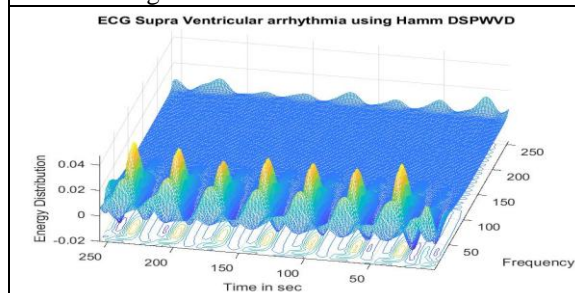


Fig. 31 Energy Distribution plot of the Supraventricular arrhythmia signal using DSPWVD with Gaussian and Hamming window functions

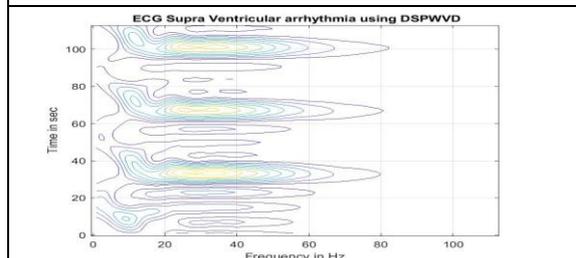


Fig. 32 Contour plot of the Supraventricular arrhythmia signal using DSPWVD with Gaussian and Hamming window functions

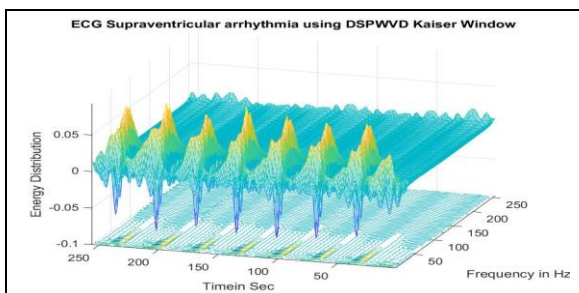


Fig. 33 Energy Distribution Plot of the Supraventricular arrhythmia signal using DSPWVD with Gaussian and Kaiser window functions

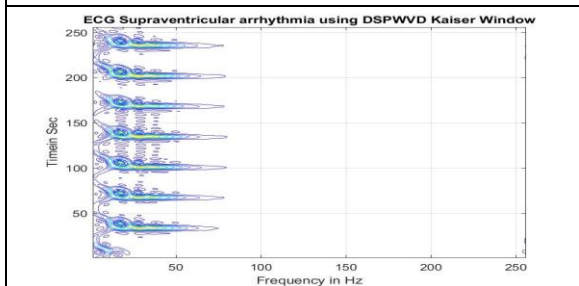


Fig. 34 Contour plot of the Supraventricular arrhythmia signal using DSPWVD with Gaussian and Kaiser window functions

From the Figs. 29-34, it was noticed that the discrete smoothed pseudo-Wigner-Ville distribution completely removed the cross-terms from the supraventricular arrhythmia signal and exhibited the changes in shape of the QRS waveform clearly with better time-frequency resolution.

Similar study was conducted for the malignant ventricular arrhythmia signal using discrete smoothed pseudo-Wigner-Ville distribution for the Hanning, Hamming and Kaiser as analysis windows and Gauss window as a smoothing window and their corresponding energy distribution and contour plots are shown in Figs. 35-40, respectively. The windows were optimized to get better frequency and time resolution as per the values given in Table. 3.

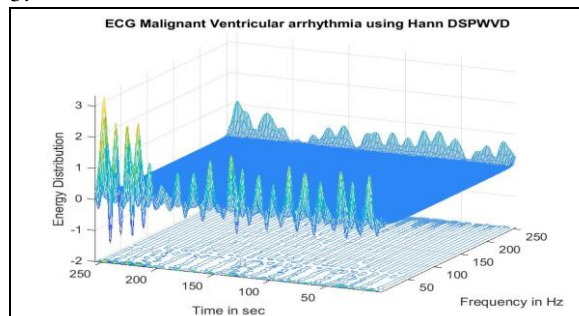


Fig. 35 Energy Distribution Plot of the Malignant ventricular arrhythmiasignal using DSPWVD with Gaussian and Hanning window functions

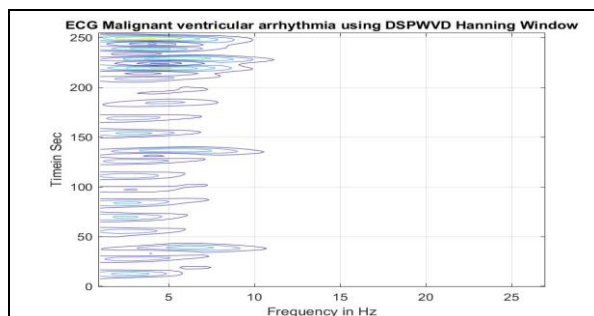


Fig 36 Contour Plot of the malignant ventricular arrhythmia signal using DSPWVD with Gaussian and Hanning window functions

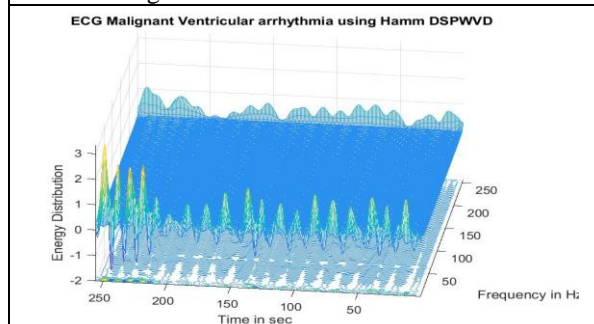


Fig. 37 Energy Distribution Plot of the Malignant ventricular arrhythmia signal using DSPWVD with Gaussian and Hamming window functions

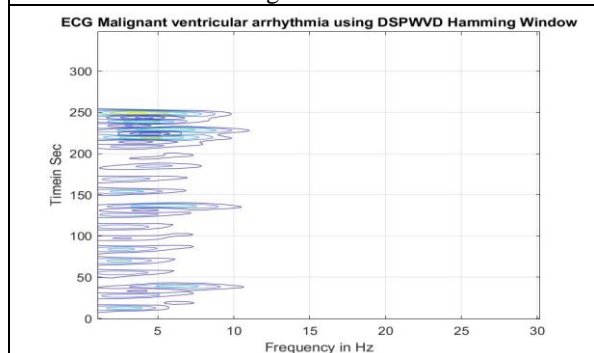


Fig 38 Contour Plot of the malignant ventricular arrhythmia signal using DSPWVD with Gaussian and Hamming window functions

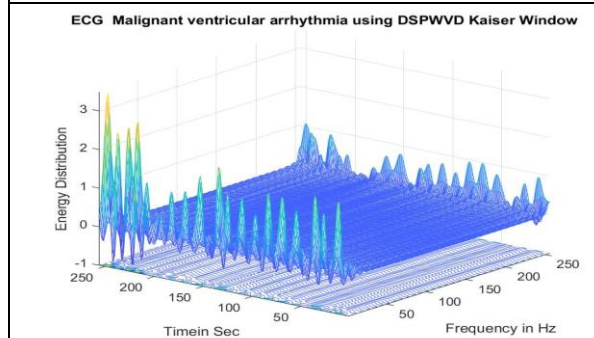


Fig. 39 Energy Distribution Plot of the Malignant ventricular arrhythmia signal using DSPWVD with Gaussian and Kaiser window functions.

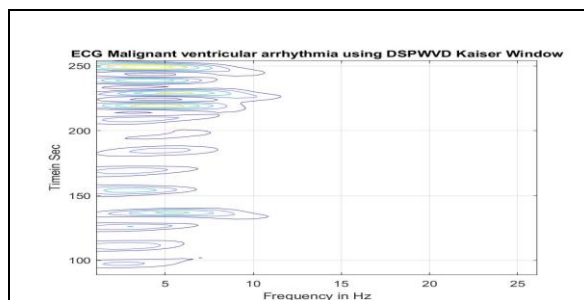


Fig. 40 Contour Plot of the malignant ventricular arrhythmia signal using DSPWVD with Gaussian and Hanning window functions

From the Figs 35-40, it is evident that the discrete smoothed pseudo-Wigner-Ville distribution completely removed the cross-term in the malignant ventricular arrhythmia signal and clearly exhibited the changes in the shape of the QRS waveform with better time-frequency resolution.

**Table 2:** Optimized window width and control parameter for supraventricular arrhythmia

Window Function	Supraventricular Arrhythmia				
	DPWVD	LI-DSWVD	DI-DSWVD	DSPWVD	
				Analysis window	Smoothing window Gaussian $G_f(u)$
Hanning	61	121	31	61	61, $\sigma=0.5$
Hamming	61	121	31	61	61, $\sigma=0.5$
Kaiser	61, $\alpha=3$	121, $\alpha=3$	63, $\alpha=3$	61, $\alpha=3$	61, $\sigma=0.5$
Gaussian	61, $\sigma=0.05$	121, $\sigma=0.5$	31, $\sigma=0.05$	--	--

**Table 3:** Optimized window width and control parameter for malignant ventricular arrhythmia

Window Function	Malignant ventricular Arrhythmia				
	DPWVD	LI-DSWVD	DI-DSWVD	DSPWVD	
				Analysis window	Smoothing window Gaussian $G_f(u)$
Hanning	61	121	31	121	63, $\sigma=0.5$
Hamming	61	121	31	121	63, $\sigma=0.5$
Kaiser	63, $\alpha=0.3$	121, $\alpha=0.3$	63, $\alpha=0.03$	63, $\alpha=0.03$	63, $\sigma=0.5$
Gaussian	61, $\sigma=0.05$	121, $\sigma=0.5$	31, $\sigma=0.05$	--	--

## VI. Conclusion

In this research work, the various forms of the discrete Wigner-Ville distributions were studied using Hanning, Hamming, Kaiser and Gaussian window function in order to improve the time-frequency resolution for better identification of the shape of the ECG waveform components. The discrete Wigner-Ville distribution computed in the time-lag domain introduced cross-term, whereas the discrete pseudo-Wigner-Ville distribution computed in the time-lag domain provided a low time-frequency resolution. Conversely, the discrete Lag-Independent smoothed Wigner-Ville distribution window function computed in the Doppler-lag domain eliminated the cross-term for the supraventricular arrhythmia signal, but it retained

the cross-term in the case of the malignant ventricular arrhythmia signal. Subsequently, the Doppler independent discrete smoothed Wigner-Ville distribution was computed in Doppler-lag domain and observed that the cross-terms were not completely removed. Finally, the discrete smoothed pseudo-Wigner-Ville distribution kernels were used as low pass filters and computed the time-frequency resolution in the Doppler-lag and time-lag domains. The analysis results revealed that the separable discrete smoothed pseudo-Wigner-Ville distribution provided a better resolution in the time-frequency domain and in turn exhibited the shape of the waveform clearly than the other time-frequency distributions. Consequently, the separable kernel time-frequency distributions may be treated as a suitable time-frequency WVD for the detection of the heart rate variability and QRS peak.

## REFERENCES

- [1]. Braham Barket and Boualem Boashash, "A High Resolution Quadratic Time-Frequency Distribution for Multicomponent Signals Analysis", IEEE Transactions on Signal Processing, Vol. 49, No. 10, October 2001.
- [2]. Boualem Boashash and Saman S. Abeysekera, "Two Dimensional Processing of Speech and ECG signals Using the Wigner-Ville Distribution", Application of Digital Image Processing IX SPIE, 1986.
- [3]. M. Wacker and H. Witte, "Time-Frequency Techniques in Biomedical Signal Analysis\* A Tutorial Review of Similarities and Differences", Methods Inf Med 2013; 52: 279-296, doi:10.3414/ME 12-01-0083
- [4]. S. Sivakumar and D. Nedumaran, "Discrete Time-Frequency Signal Analysis and Processing Techniques for Non-Stationary Signals", Journal of Applied Mathematics and Physics, 2018, Vol. 6, pp. 1916-1927. ISSN online:2327-4379, doi:10.4236/jamp.2018.69163.
- [5]. S.GokhunTanyer, Gorkem and Peter Driessen, "High Resolution Time-frequency Analysis of Non-Stationary Signals", Proceedings of the 4<sup>th</sup> International Conference of Control, Dynamic Systems, and Robotics (CDSR'17) Toronto, Canada – August 21 – 23, 2017, Paper No.126. doi:10.11159/cdsr17.126.
- [6]. Boualem Boashash and Peter J. Black, "An Efficient Real-Time Implementation of the Wigner-Ville Distribution", IEEE Transactions on Acoustics, Speech and Signal Processing, vol. ASSP-35, No 11 November 1987.
- [7]. Zhongguo Liu, Changchun Liu, BoqiangLiu, Yangsheng L, Yinsheng Lei and

- Mengsun Yu1," Self Spectrum Window Method in Wigner-Ville Distribution", Proceedings of the 2005 IEEE, Engineering in Medicine and Biology 27th Annual Conference, Shanghai, China, September 1-4, 2005
- [8]. T.A.C. M.Claasen and W.F.G. Mecklenbrauker, "The Wigner Distribution – A Tool for Time-Frequency Signal Analysis", Philips Journal of Research. Vol.35, No. 6, pp. 372-389, 1980.
- [9]. S. E. Qian and D. P. Chen, Joint time-frequency analysis: methods and applications (Upper Saddle River, NJ: Prentice Hall PTR, 1996) pp. 203-235.
- [10]. F. S. Yang, Y. S. Lu, Biomedical signal processing and recognition (Tianjin Science & Technology Translation & Publishing Co., 1997), pp. 224-284.
- [11]. Z. Lin, and J. D. Chen, "Advances in time-frequency analysis of biomedical signals", Crit Rev Biomed Eng, vol.24, no. 1, pp. 1-72 Jan 1996.
- [12]. Y. S. Yan, C. C. Poon, and Y. T. Zhang, "Reduction of motion artifact in pulse oximetry by Smoothed Pseudo Wigner-Ville Distribution," J Neuroengineering Rehabil, vol. 2, no. 1, pp. 3, Mar 2005.
- [13]. S. Ghofrani, A. Ayatollahi, and M. B. Shamsollahi, "Wigner-Ville distribution and Gabor Transform in Doppler Ultrasound Signal Processing," Biomed Sci Instrum, vol. 39, pp. 142-147, Jan. 2003.
- [14]. E. Pereira, M. A. Custaud, J. Frutoso, L. Somy, C. Gharib, and J. O. Fortrat, "Smoothed Pseudo -Wigner-Ville distribution as an alternative to Fourier transform in rats," Auton Neurosci, vol. 87, no. 2-3, pp. 258-67, Mar 2001.
- [15]. Andria G.M. Savino, " Interpolated Smoothed Pseudo Wigner-Ville Distribution for Accurate Spectrum Analysis", IEEE Trans. on Instrumentation and Measurement. 45(4): 818-823.
- [16]. Roshan Joy Marits U. Rajendra Acharya and Hojjat Adeli, "Current Methods in Electrocardiogram Characterization", Computers in Biology and Medicine, doi:10.1016/j.combiomed.2014.02.012, 2014 Elsevier.
- [17]. A. Dliou, R. Latif and M. Laaboubi, "Arrhythmia ECG Signal Analysis using Non Parametric Time-Frequency Techniques", International Journal of Computer Applications (0975 - 8887) Vol. 41 - N0.4. March 2012.
- [18]. Allam Mousa and Rashid Saleem, "The Shortage of WVD in Analyzing Abnormal ECG Signal", IEEE Symposium on Industrial Electronics and Applications (ISIEA 2010), October 3-5, 2010, Penang, Malaysia.
- [19]. Physiobank, Physionet, Physiologic Signal Archives for Biomedical Research, [http://www.physionet.org/physio\\_bank](http://www.physionet.org/physio_bank).
- [20]. Boualem Boashash, "Note on the Use of the Wigner Distribution for Time-Frequency Signal Analysis", IEEE, Transaction on Acoustics, Speech and Signal Processing, vol. 36, No.9, pp. 1518-1521, September 1988.
- [21]. S. Lawrence Marple, Jr., "Computing the Discrete-Time "Analytic" Signal via FFT", IEEE Transactions On Signal Processing, Vol. 47, No. 9, September 1999
- [22]. B. Boashash, Time-frequency signal analysis, in: Advances in Spectral Analysis and Array Processing (Prentice Hall, 1991), pp.418-517, <http://qspace.qu.edu.qa/handle/10576/10832>.
- [23]. Pierre Wickranarachi, "Effects of Windowing on the Spectral Content of a Signal", Sound and Vibration, January 2003.
- [24]. Shaila D. Apte, Advanced Digital Signal Processing (Wiley, First Edition, 2013), pp.128-132.
- [25]. J. O' Toole and B. Boashash, "Optimization of the Realization of Quadratic Discrete Time-Frequency Distributions as a MATLAB Toolbox", In Proceedings International Conference on Scientific and Engineering Computation, Singapore, 2004.
- [26]. Boualem Boashash, Ghasem Azemi and John M. O'Toole, "Time-Frequency Processing of Non-stationary Signals", IEEE, Signal Processing Magazine, pp. 108 -119, November 2013
- [27]. T.A.C.M. Claasen and W.F.G. Mecklenbrauker, "The Wigner Distribution - A Tool for Time-Frequency Signal Analysis Part-III: Relations with Other Time-Frequency Signal Transformations", Philips J.Res.35, 372-389, 1980.
- [28]. Gerald Matz and Franz Hlawatsch, "Wigner Distributions (nearly) Everywhere: Time-Frequency Analysis of Signals, Systems, Random Processes, Signal Spaces and Frames", Signal Processing, Vol. 83, 2003, pp. 1355-1378, doi: 10.1016/S0165-1684(03)00086-0.
- [29]. P. Kotsas, C. Pappas, M. Strintzis and N. Maglaveras, Non-stationary ECG Analysis Using Wigner-Ville Transforms and Wavelets, 1993 IEEE.
- [30]. Boualem Boashash and Peter J. Black, "An Efficient Real-Time Implementation of the Wigner-Ville Distribution", Transactions on Acoustics, Speech, and Signal Processing, Vol. ASSP-35, No. 11. November 1987.

- [31]. Sanjit K. Dash and G. Sasibhushana Rao, "A Comparative Study of Pseudo-Wigner-Ville Distribution (PWVD), WVD and STFT in ECG Signal Analysis", *International Journal of Advanced Research in Electrical, Electronics and Instrumentation Engineering*, vol. 6, Issue 9, pp. 6899-6910, September 2017, doi:10.15662/IJAREEIE.2017.0609038.
- [32]. Ahmad ZuriSha' Ameri and Boualem Boashash, "The Lag Windowed Wigner-Ville Distribution: An Analysis Method for HF Data Communication Signals", *FurnalTeknologi* 30 ID: 33-54 (C) Universiti Teknologi Malaysia.
- [33]. K.M.M. Prabhu and R. Shanmugasundaram, "Fast Algorithm for Pseudo-discrete Wigner-Ville Distribution using Moving Discrete Hartley Transform", *IEEE Proc.-Vis. Image Signal Processing*, Vol. 143, No. 6, December 1996.
- [34]. Young S.Shin and Jae-Jin Jeon, "Pseudo Wigner-Ville Time-Frequency Distribution and its Application to Machinery Condition Monitoring", *Shock and Vibration*, vol. 1, pp. 65-76, 1993
- [35]. Cher Ming Tan, and Shin Yeh Lim, "Application of Wigner Ville Distribution in Electro-migration Noise Analysis", *IEEE Transactions on Device and Materials Reliability*, vol. 2, No. 2, June 2002.
- [36]. Boualem Boashash and Samir Ouelha, "Efficient software platform TFSAP 7.1 and Matlab package to compute Time-Frequency Distributions and related Time-Scale methods with extraction of signal characteristics", *Journal of SoftwareX*, 2017, <http://dx.doi.org/10.1016/j.softx.2017.08.003>
- [37]. Boualem Boashash, LarbiBoubchir and GhasemAzemi, "A Methodology for the time-Frequency Image Processing Applied to the Classification of Non-Stationary Multichannel Signals Using Instantaneous Frequency Descriptors with Application to Newborn EEG Signals", *EURASIP Journal on Advances in Signal Processing* 2012.
- [38]. Boualem Boashash and Taoufik Ben-Jabeur, "Design of A High-Resolution Separable-Kernel Quadratic TFD for Improving Newborn Health Outcomes Using Fetal Movement Detection", *The 11th International Conference on Information Sciences, Signal Processing and their Applications*, IEEE pp. 354-359, 2012
- [39]. Boualem Boashash, Nabeel AliKhan and Taoufik Ben-Jabeur, "Time-frequency features for pattern recognition using high-resolution TFDs: A tutorial review" *Journal of Digital Signal Processing*, 2015, doi: 10.1016/j.dsp.2015.12.015
- [40]. Abdelghani Djebbari and F. Bereksi-Reguig, "Smoothed Pseudo Wigner-Ville Distribution of Normal and Aortic Stenosis Heart Sounds", *Journal of Mechanics in Medicine and Biology*, vol. 5, No. 3 (2005) 415-428, [www.worldscientific.com](http://www.worldscientific.com).
- [41]. Guoqing Liu, Xi Zhang and Oibing Lv, "The Realization of Smoothed Pseudo Wigner-Ville Distribution Based on Lab View", *Applied Mechanics and Materials*, ISSN:1662-7482, Vols. 239-240, pp. 1493-1496, doi:10.4028/www.scientific.net/AMM 239-240,1493